GEOPHYSICAL RESEARCH LETTERS, VOL. 40, 2055–2059, doi:10.1002/grl.50397, 2013

Characterizing groundwater flow and heat transport in fractured rock using fiber-optic distributed temperature sensing

T. Read,[1] O. Bour,[2] V. Bense,[1] T. Le Borgne,[2] P. Goderniaux,[2,3] M.V. Klepikova,[2] R. Hochreutener,[2] N. Lavenant,[2] and V. Boschero[2]

Received 11 February 2013; revised 19 March 2013; accepted 20 March 2013; published 23 May 2013.

[1] We show how fully distributed space-time measurements with Fiber-Optic Distributed Temperature Sensing (FO-DTS) can be used to investigate groundwater flow and heat transport in fractured media. Heat injection experiments are combined with temperature measurements along fiber-optic cables installed in boreholes. Thermal dilution tests are shown to enable detection of cross-flowing fractures and quantification of the cross flow rate. A cross borehole thermal tracer test is then analyzed to identify fracture zones that are in hydraulic connection between boreholes and to estimate spatially distributed temperature breakthrough in each fracture zone. This provides a significant improvement compared to classical tracer tests, for which concentration data are usually integrated over the whole abstraction borehole. However, despite providing some complementary results, we find that the main contributive fracture for heat transport is different to that for a solute tracer. **Citation:** Read, T., O. Bour, V. Bense, T. Le Borgne, P. Goderniaux, M. V. Klepikova, R. Hochreutener, N. Lavenant, and V. Boschero (2013), Characterizing groundwater flow and heat transport in fractured rock using Fiber-Optic Distributed Temperature Sensing, *Geophys. Res. Lett.*, *40*, 2055–2059, doi:10.1002/grl.50397.

1. Introduction

[2] Heterogeneous aquifers, such as fractured rocks, often require detailed characterization for water resources assessment and for the prediction of potential contaminant pathways [*Neuman*, 2005]. Such characterization may consist of simply identifying the most transmissive fractures to the formulation of a statistical model of the solute transport properties of the fracture network such as permeability and dispersivity. This is usually carried out in situ through cross-flowmeter tests or hydraulic response tests [*Paillet*, 1998; *Illman et al.*, 2009], or with tracer experiments using solutes. In between two or more boreholes, tracer tests allow the advective velocity and dispersion of solutes to be quantified [e.g., *Becker and Shapiro*, 2003]. While these well-established aquifer characterization techniques successfully yield results in terms of flow through the fracture network, the requirement for frequent sampling and subsequent analysis may be time consuming and expensive. Only with sophisticated multi-depth sampling, multi packer systems, or repetitive continuous logging, can a more continuous log along the borehole be obtained. This, as opposed to a time series recorded at a single depth that incorporates the response of all transmissive features intersecting the borehole, is required for the analysis of the transport properties through individual fracture zones or permeable units. There is, therefore, a great need for new sensors capable of providing continuous measurements in space and time.

[3] The availability of fully distributed fiber-optic temperature sensors (FO-DTS) allows such continuous measurements for temperature [*Selker et al.*, 2006; *Tyler et al.*, 2009]. It is long-established that heat can be used as a tracer to estimate groundwater flow in a range of hydrogeological settings [*Anderson*, 2005]. Heat is more diffuse than solutes by several orders of magnitude, but in some cases, has been shown to be a reasonable proxy for solute tracers and hence can be used to calibrate models of hydraulic conductivity distribution [*Ma et al.*, 2012]. In fractured media, heat may be expected to bring different and complementary information compared to solute tracers, since it is much more sensitive to matrix diffusion processes [*Geiger and Emmanuel*, 2010].

[4] The application of FO-DTS has been demonstrated in boreholes for thermal conductivity estimation and surface temperature reconstruction [*Freifeld et al.*, 2008]. FO-DTS was also used to infer fluid flow rates inside boreholes as an alternative for a directly measured flow log [*Leaf et al.*, 2012]. In the application of aquifer characterization as described above, FO-DTS deployments have been limited to only a few case studies [*Hurtig et al.*, 1994; *Macfarlane et al.*, 2002], and there have been significant advances in the measurement precision of FO-DTS systems in the intervening time. Here, we demonstrate the potential for FO-DTS monitoring of heat dilution and tracer tests in heterogeneous systems such as fractured rock aquifers. We show how cross flow rates from fracture zones and temperature breakthrough curves for individual fractures can be calculated and find that FO-DTS offers some significant advantages over point temperature loggers for monitoring such tests and for characterizing flow and heat transport in fractured rocks.

2. Methodology

[5] Thermal test data were collected at Ploemeur, Brittany, northwest France, in four boreholes (B1, B2, B3, and F22), separated by a distance of 6 to 30 m and ranging from 70 to 100 m deep (Figure 1). The geology of the site

[1]School of Environmental Sciences, University of East Anglia, Norwich, UK.
[2]Géosciences Rennes (UMR 6118), University of Rennes 1, Rennes, France.
[3]Department of Geology and Applied Geology, University of Mons, Mons, Belgium.

Corresponding author: T. Read, School of Environmental Sciences, University of East Anglia, Norwich, UK. (Tom.read@uea.ac.uk)

0094-8276/13/10.1002/grl.50397

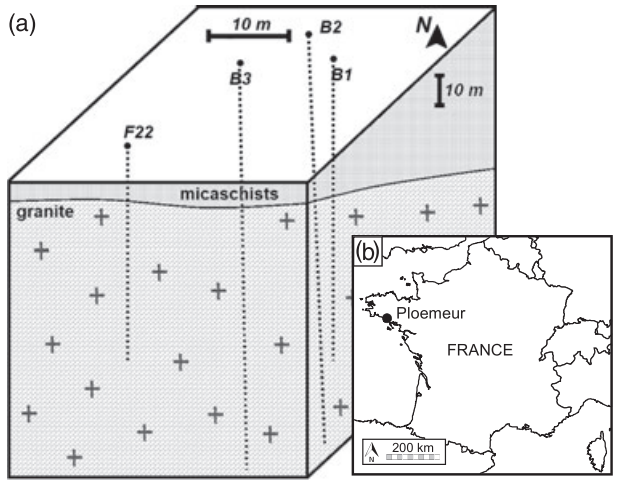

Figure 1. (a) Borehole array configuration and (b) location of the site.

consists of mica-schist, underlain by an intrusive granite, the contact of which provides a locally significant groundwater resource [*Le Borgne et al.*, 2004; *Ruelleu et al.*, 2010]. The site is considered a typical fractured crystalline basement aquifer and has been subject to numerous hydraulic [*Le Borgne et al.*, 2004, 2007], and geophysical tests [e.g., *Dorn et al.*, 2012]. Interference tests have suggested that fluid flow and associated tracer transport between boreholes are concentrated in only a few transmissive fracture zones [*Le Borgne et al.*, 2007]. Solute dispersion is dominated by fracture network connectivity showing that few interconnecting fractures contribute to solute transport at the scale of several meters by which the boreholes are separated [*Dorn et al.*, 2012].

[6] For the FO-DTS experiments discussed here, a single BruSteel (Brugg Cables, Switzerland) steel armored fiber-optic cable of 1 km in length was installed in all four boreholes for the continuous monitoring of temperature. Additionally, two coiled sections of cable were placed in a calibration bath consisting of water wetted ice and monitored with a submersible temperature logger. We deploy the widely used Oryx-DTS unit (Sensornet Ltd., UK, Herts), configured to take single-ended temperature measurements with a spatial sampling interval of 1.01 m along the cable and an integration time of 2 min. To convert the laser backscatter detected by the instrument to a temperature, we post-processed the raw backscatter data to further improve the instrument accuracy using the dynamic calibration procedure outlined by *Hausner et al.* [2011]. However, this was not possible for the thermal dilution tests due to warming of the ice baths; so here, we rely on the inbuilt calibration software of the device.

2.1. Thermal Dilution Test Set-Up

[7] Thermal dilution tests were conducted in borehole B3. The method we employ is similar to a borehole dilution test using solutes [e.g., *Novakowski et al.*, 2006; *Brouyère et al.*, 2008], but here using heat instead. A similar method has been applied in lined boreholes using the Active Line Source technique [*Pehme et al.*, 2007]. Since we are interested in cross flowing fractures, an inflatable packer was installed at a depth of 44 m to prevent ambient vertical flow in between fractures tapping into the borehole which otherwise occurs in most boreholes at the site. We injected water, heated to 50°C using a mobile heating system, just above the packer at 43 m. The borehole was pumped at the same rate at shallow depth in order to draw the warm injected water upwards. During the experiment, the hydraulic head in the borehole was monitored to verify that any changes were small enough to ensure no net flow in or out of the borehole, taking into account effects of temperature on fluid density. The thermal dilution test was carried out under ambient conditions and then under cross pumping conditions, with B2 at a distance of 10 m pumped at 140 L min^{-1}.

2.2. Thermal Tracer Test Set-Up

[8] For the thermal tracer test, we concentrate on B1, the injection well, and B2, the abstraction well, separated by approximately 6 m. Two inflatable packers were used to hydraulically isolate a known fracture at a depth of 78.7 m in B1 (B1-79). Water was injected into a 1-m interval across this fracture at a constant rate and temperature of 35 L min^{-1} and 50°C. Simultaneously, B2 was pumped at a constant rate of 140 L min^{-1}. The injection of heated water in B1 continued for approximately 11 h and was followed by a "push" of water at ambient groundwater temperature for 5 h to test the heat recovery under similar hydraulic conditions. Subsequently, the injection at B1 ceased but pumping in the abstraction well, B2, continued. In addition to monitoring by FO-DTS, temperature in the abstraction well was recorded continuously using three temperature loggers located at set depths of 40, 60, and 72 m.

3. Results

3.1. Thermal Dilution Tests

[9] FO-DTS data for the thermal dilution tests carried out in B3, including both the injection and cooling phases, are shown in Figures 2a and 2c for ambient and cross pumping conditions, respectively. In both cases, $t = 0$ h corresponds to when the injection stopped. By the time the injection ceases, the fluid between the point of injection and abstraction is replaced with water approximately 25 to 40°C warmer than ambient temperatures. During the cooling phase, the absolute temperature values are clearly influenced by the initial conditions at 0 h which were not entirely isothermal. To correct for the influence of the initial non-isothermal distribution of heat in the borehole on the depth-variant cooling rates observed later, the Relative Temperature Anomaly (*RTA*) was calculated according to

$$RTA(z,t) = \frac{T(z,t) - T_{ambient}(z)}{T_{initial}(z) - T_{ambient}(z)} \quad (1)$$

where $T_{ambient}$ is the temperature prior to the start of the injection and $T_{initial}$ is the temperature when the injection ceased. This scales the initial temperature anomaly to unity at all depths, with a value of zero representing a full return to pretesting ambient temperature conditions. The cased section cools more slowly than the open section below, which can be explained by the larger borehole diameter and low thermal conductivity casing material. From the end of the casing to 36 m, the cooling is relatively uniform, which corresponds well with core data and flow logs that suggest there are no significant transmissive fractures intersecting the borehole along this depth interval (Figures 2b and 2d). A zone of enhanced cooling beneath 36 m can be readily distinguished

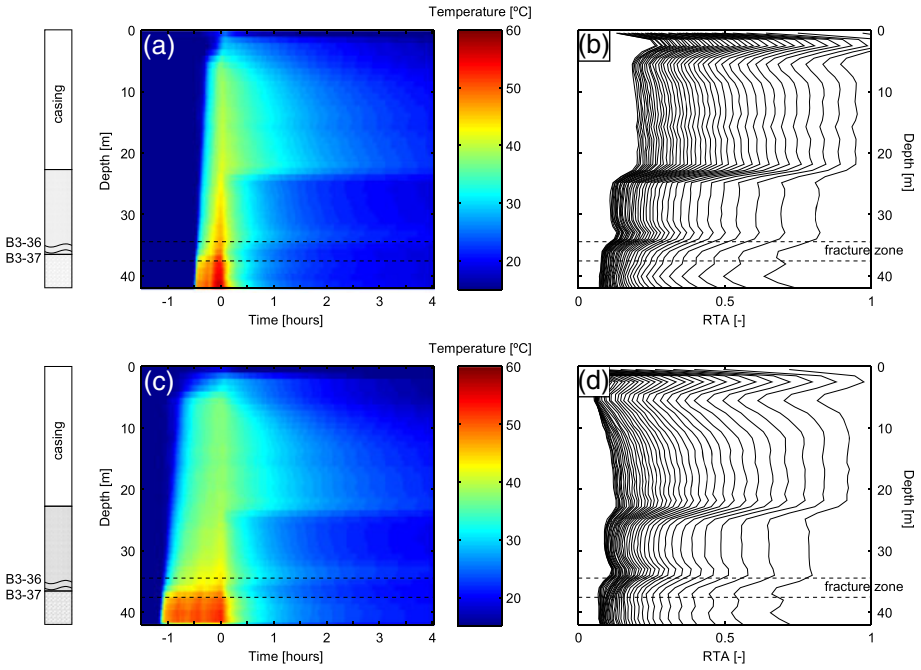

Figure 2. Temperature in B3 during the thermal dilution test under (a) ambient conditions and (c) while pumping B2, and (b) corresponding Relative Temperature Anomaly and (d) at normalized times of 0.2 to 8 [-] (right to left). The time was normalized to account for the different injection durations, with 1 h taken as the standard injection length.

in ambient and cross pumping conditions. The top of this zone coincides with two transmissive fractures located just above the transition from mica-schist to granite identified by *Le Borgne et al.* [2007] and continues to 42 m.

[10] The fast cooling below 36 m is potentially due to both advective flow in the fracture zone, and also partly to the higher thermal diffusivity of granite compared to mica-schist (1.8×10^{-6} and 1.4×10^{-6} $m^2 s^{-1}$, respectively). Nevertheless, during the injection phase, in particular during cross-pumping (Figure 2c), the injected water is cooled significantly as it passes the fracture zone. During this time, the contrast in temperature across the fracture zone would not be explained by the contrast in thermal diffusivity between granite and mica-schist. In the following, we assume that during the injection phase, this step-like change in temperature across the fracture zone is due solely to an advective effect.

[11] To estimate the cross-flow rate Q_f [L min^{-1}] through the fracture zone, we use a mixing equation applicable during the injection phase:

$$Q_f = \left(\frac{T_{below} - T_{above}}{T_{above} - T_f} \right) Q_{inject} \qquad (2)$$

in which Q_{inject} [L min^{-1}] is the rate of injection, and T_{above} and T_{below} are the temperatures above and below the fracture zone of interest, respectively, and T_f is the temperature of groundwater flowing through the fracture zone, which is assumed to be constant with time. This mixing equation assumes that water from the cross flowing fracture enters the borehole and becomes fully mixed before being advected upwards or leaving the borehole. Application of equation (2) using the FO-DTS data for B3 and a T_f of 15°C results in a calculated cross flow of 3.4 L min^{-1} for the fracture zone at 36 m. When the thermal dilution test was repeated, but under cross pumping conditions, the calculated flow through this zone increases to 3.9 L min^{-1}, a slight but measurable change. Hence, using FO-DTS to monitor thermal dilution tests allowed us to measure significant ambient flow through the identified fracture. The ambient flow measured through the fracture is quantitatively comparable with the vertical ambient flows measured by precise borehole flowmeters [*Le Borgne et al.*, 2007]. Such ambient flows are explained by the location of the site in a discharge area of the catchment. The effect of pumping in an adjacent well, although small, apparently produces a temperature effect strong enough to be detected.

3.2. Thermal Tracer Tests

[12] Time series of temperature data from the temperature loggers and corresponding post-processed FO-DTS measurements at these depths during the thermal tracer test are shown in Figure 3a. The data show good agreement with the FO-DTS data having high temporal repeatability characterized by a standard deviation of 0.03°C. Thus, the FO-DTS appears to be an excellent tool for detecting and monitoring temperature change during thermal tracer tests.

[13] FO-DTS data for all depths in the abstraction well are shown in Figure 3b in terms of a temperature breakthrough, calculated as the difference between the measured temperature and the mean of the 10 temperature-depth profiles obtained prior to the injection of heated water. Based on visual inspection of the temperature data alone, there are three readily identifiable fractures contributing to the upflow in the borehole to the pump. At approximately 79 and then 67 m, there are sources of warmer water that must therefore be fracture zones that are in connection with the fracture zone B1-79 in the injection well. Between 57 and 59 m, there appears to be a wider zone of fracture inflows that results in the cooling of the upflowing borehole water and therefore appear to be disconnected from B1-79. From this point upwards, there appear to be no thermal breakthroughs.

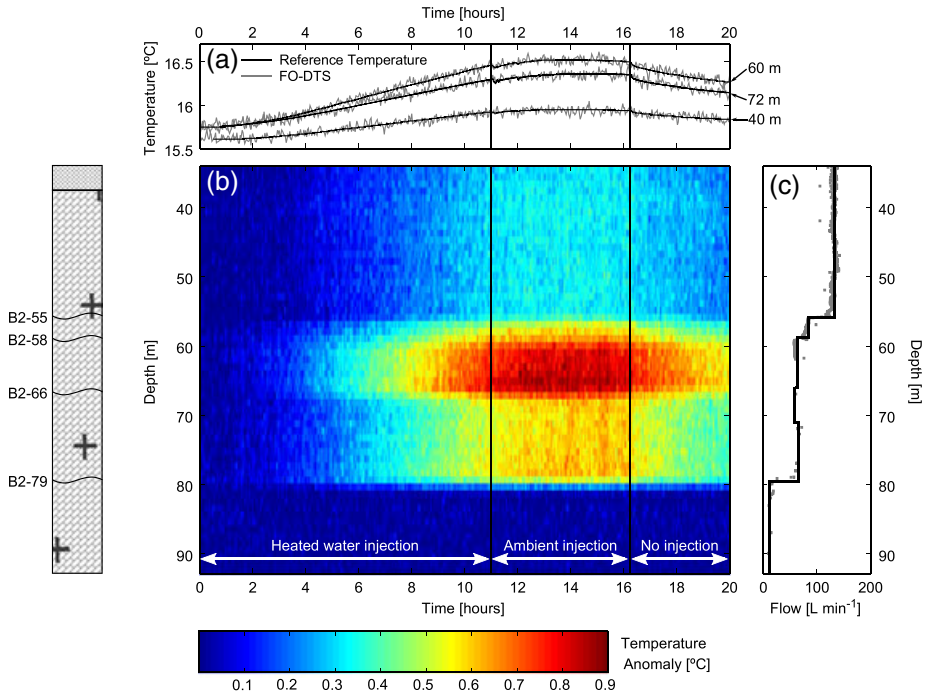

Figure 3. (a) Temperature logger and DTS measured temperature at the corresponding depths during the thermal tracer test from B1 to B2, (b) DTS measured temperature anomaly for all depths, and (c) measured flow in B2 for a pumping rate of 140 L min^{-1} with solid line to indicate the flow profile assumed for the application of equation (3).

[14] In the following, we estimate the contribution of each fracture to the transport of heat during the thermal tracer test and compare it to other tracer tests. Applying a simple conservative mixing equation, the temperature of groundwater entering the borehole from a fracture zone is given by:

$$T_f = \frac{Q_{above}T_{above} - Q_{below}T_{below}}{Q_{above} - Q_{below}} \quad (3)$$

For this calculation, the FO-DTS measured temperature in B2 was combined with flowmeter data (Figure 3c). The high frequency noise in the FO-DTS data, which would otherwise be amplified (approximately 0.1°C), was removed by fitting a second degree polynomial using a weighted linear least-squares regression to each of the thermal breakthrough curves along the borehole length. The flow log indicated that there was no detectable inflow at 66 m where the largest step change in temperature was observed, whereas two closely spaced fractures can be seen in an optical borehole log in this zone. For the purpose of the thermal breakthrough calculation, we assume that the fractures contribute 5 L min^{-1} as this is approximately the detection limit of the impeller flowmeter for the borehole diameter. The true temperature breakthrough from this fracture zone is likely to be higher than calculated in the following, as the flow from this fracture is potentially much less than this.

[15] Using equation (3), Figure 4 provides the calculated temperature of the inflow to B2 from each fracture zone. The largest temperature response (4.0°C) is from fracture B2-66. This breakthrough is very rapid and continues for approximately 1 h after the injection switched to a cold water push. In comparison, B2-79 responds more slowly and rises to a lower temperature (0.8°C). The calculated responses for fracture zones B2-58 and B2-55 confirm the initial observation that no heat was recovered from these fractures during the duration of the experiment.

[16] Compared to solute tracer tests, performed at the same location, the main differences observed are the time, amplitude, and spatial distribution of the breakthrough. For instance, with a slug injection of the fluorescent dye uranine, the peak arrives at B2 after around 20 min, but only very slight changes are observed at these times using heat as a tracer (Figure 4). Thus, the thermal breakthrough is significantly attenuated due to fracture-matrix heat exchange.

[17] *Dorn et al.* [2012] carried out a solute tracer test between B2 and B1 by injecting a saline tracer into the same

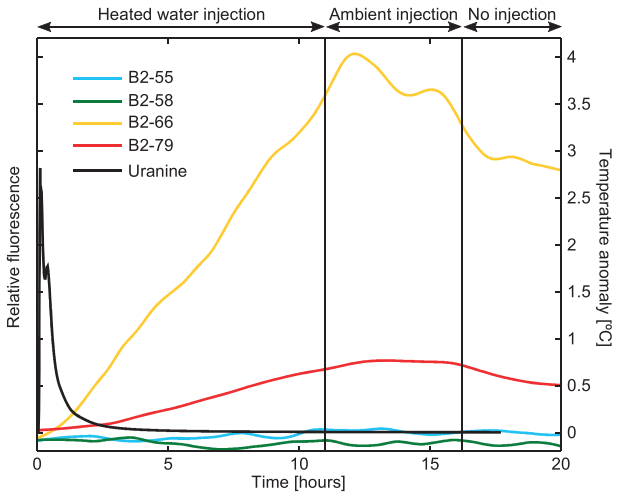

Figure 4. Uranine breakthrough and calculated temperature anomaly of the inflowing fractures B2-55, B2-58, B2-66, and B2-79 during the thermal tracer test.

fracture and pumping B2 at a rate of 30 L min^{-1}. During their test, the main contributing fracture in B2 was B2-79 [*Dorn et al.*, 2012, Figures 5 and 7]. Fracture B2-66 was detected in the ground-penetrating radar time-lapse images [*Dorn et al.*, 2012, Figure 10a], but did not contribute significantly to conductivity variations in the borehole. For the duration of our thermal test, the main contributive fracture was B2-66. These differences are significant as they confirm that thermal and solute tracer tests do not provide the same information on the transport pathways, even at the scale of a few meters. This could be explain by density effects that would drive the saline tracer downwards and heat upwards, while in addition, heat transfer is much more sensitive to fracture-matrix exchanges compared to solute transfer. Flow channeling may also be a factor since it may reduce the fracture-matrix exchange area [e.g., *Neuville et al.*, 2010]. In the present case, fracture B2-66 may be of a small aperture, with strongly channelized flow, that would explain a negligible flow contribution and only small solute tracer recovery but an important temperature breakthrough as we observe.

4. Conclusions

[18] We find that FO-DTS is significantly advance over the traditional point temperature sensors in the borehole environment that enables thermal dilution or thermal tracer tests to be monitored accurately and efficiently in both time and space. Such thermal experiments offer new insights in the characterization of fractured media, as they provide complementary information with respect to solute tracer experiments. In particular, the thermal dilution test was shown to be an efficient method to estimate cross flowing groundwater through a fracture zone.

[19] FO-DTS was also found very useful to provide a detailed characterization of heat transport through a fracture network. The thermal breakthrough curve is strongly attenuated due to fracture-matrix interactions, and the relative contribution of the different fractures is found to be strikingly different than for solute transport potentially due to channeling and density effects. For this application, the main advantages of FO-DTS are that it avoids the risk of disturbing the fluid column by raising and lowering a probe, and it generates a synchronous data set with measurements distributed over the entire borehole. Hence, we anticipate that FO-DTS combined with heating experiments will become a more commonplace geophysical method for aquifer characterization.

[20] **Acknowledgments.** Funding for this work was provided by the INTERREG IV project CLIMAWAT, Marie Curie ITN project IMVUL, the national network of hydrogeological sites H+, and a Natural Environment Research Council (NERC) studentship (NE/J500069/1) to Tom Read. The authors thank Alain Dassargues and S. Brouyère from the Université de Liegè for generously lending the portable water heater. We would also like to thank the two reviewers for their constructive comments.

[21] The Editor thanks Matthew Becker and Niklas Linde for their assistance in evaluating this paper.

References

Anderson, M. P. (2005), Heat as a ground water tracer, *Ground Water*, *43*(6), 951–68, doi:10.1111/j.1745-6584.2005.00052.X.

Becker, M. W., and A. M. Shapiro (2003), Interpreting tracer breakthrough tailing from different forced-gradient tracer experiment configurations in fractured bedrock, *Water Resour. Res.*, *39*(1), 1024, doi:10.1029/2001WR001190.

Brouyère, S., J. Batlle-Aguilar, P. Goderniaux, and A. Dassargues (2008), A new tracer technique for monitoring groundwater fluxes: The finite volume point dilution method, *J Contam. Hydrol.*, *95*(3-4), 121–40, doi:10.1016/j.jconhyd.2007.09.001.

Dorn, C., N. Linde, T. Le Borgne, O. Bour, and M. Klepikova (2012), Inferring transport characteristics in a fractured rock aquifer by combining single-hole ground-penetrating radar reflection monitoring and tracer test data, *Water Resour. Res.*, *48*, W11521, doi:10.1029/2011WR011739.

Freifeld, B. M., S. Finsterle, T. C. Onstott, P. Toole, and L. M. Pratt (2008), Ground surface temperature reconstructions: Using in situ estimates for thermal conductivity acquired with a fiber-optic distributed thermal perturbation sensor, *Geophys. Res. Lett.*, *35*, L14309, doi:10.1029/2008GL034762.

Geiger, S., and S. Emmanuel (2010), Non Fourier thermal transport in fractured geological media, *Water Resour. Res.*, *46*, W07504, 1–13, doi:10.1029/2009WR008671.

Hausner, M. B., F. Suárez, K. E. Glander, N. V. D. Giesen, J. S. Selker, and S. W. Tyler (2011), Calibrating single-ended fiber-optic Raman spectra distributed temperature sensing data, *Sensors*, *11*(11), 10,859–10,879, doi:10.3390/s111110859.

Hurtig, E., S. Großwig, M. Jobmann, K. Kuhn, and P. Marschall (1994), Fibre-optic temperature measurements in shallow boreholes: Experimental application for fluid logging, *Geothermics*, *23*(4), 355–364.

Illman, W. A., X. Liu, S. Takeuchi, T.-C. J. Yeh, K. Ando, and H. Saegusa, (2009), Hydraulic tomography in fractured granite : Mizunami underground research site, Japan, *Water Resour. Res.*, *45*, W01406, doi:10.1029/2007WR006715.

Le Borgne, T., O. Bour, J. R. de Dreuzy, P. Davy, and F. Touchard (2004), Equivalent mean flow models for fractured aquifers: Insights from a pumping tests scaling interpretation, *Water Resour. Res.*, *40*, W03512, doi:10.1029/2003WR002436.

Le Borgne, T., et al. (2007), Comparison of alternative methodologies for identifying and characterizing preferential flow paths in heterogeneous aquifers, *J. Hydrol.*, *345* (3-4), 134–148, doi:10.1016/j.jhydrol.2007.07.007.

Leaf, A. T., D. J. Hart, and J. M. Bahr (2012), Active thermal tracer tests for improved hydrostratigraphic characterization, *Ground Water*, *50*(5), 726–735, doi:10.1111/j.1745-6584.2012.00913.X.

Ma, R., C. Zheng, J. M. Zachara, and M. Tonkin (2012), Utility of bromide and heat tracers for aquifer characterization affected by highly transient flow conditions, *Water Resour. Res.*, *48*, W08523, doi:10.1029/2011WR011281.

Macfarlane, A., A. Förster, D. Merriam, J. Schrötter, and J. Healey (2002), Monitoring artificially stimulated fluid movement in the Cretaceous Dakota aquifer, western Kansas, *Hydrogeol. J.*, *10*(6), 662–673.

Neuman, S. P. (2005), Trends, prospects, and challenges in quantifying flow and transport through fractured rocks, *Hydrogeol. J.*, *13*, 124–147, doi:10.1007/s10040-004-0397-2.

Neuville, A., R. Toussaint, and J. Schmittbuhl (2010), Hydrothermal coupling in a self-affine rough fracture, *Phys. Rev. E*, *82*, 036317, doi:10.1103/PhysRevE.82.036317.

Novakowski, K., G. Bickerton, P. Lapcevic, J. Voralek, and N. Ross (2006), Measurements of groundwater velocity in discrete rock fractures, *J. Contam. Hydrol.*, *82*, 44–60, doi:10.1016/j.jconhyd.2005.09.001.

Paillet, F. L. (1998), Flow modeling and permeability estimation using borehole flow logs in heterogeneous fractured formations, *Water Resour. Res.*, *34*(5), 997–1010, doi:10.1029/98WR00268.

Pehme, P. E., J. P. Greenhouse, and B. L. Parker (2007), The active line source temperature logging technique and its application in fractured rock hydrogeology, *J. Environ. Eng. Geoph.*, *12*(4), 307–322, doi:10.2113/JEEG12.4.307.

Ruelleu, S., F. Moreau, O. Bour, D. Gapais, and G. Martelet (2010), Impact of gently dipping discontinuities on basement aquifer recharge: An example from Ploemeur (Brittany, France), *J. Appl. Geophys.*, *70*(2), 161–168, doi:10.1016/j.jappgeo.2009.12.007.

Selker, J. S., et al. (2006), Distributed fiber-optic temperature sensing for hydrologic systems, *Water Resour. Res.*, *42*, W12202, doi:10.1029/2006WR005326.

Tyler, S. W., J. S. Selker, M. B. Hausner, C. E. Hatch, T. Torgersen, C. E. Thodal, and S. G. Schladow (2009), Environmental temperature sensing using Raman spectra DTS fiber-optic methods, *Water Resour. Res.*, *45*, W00D23, doi:10.1029/2008WR007052.